

## Seasonal Freezing Effects on the Lateral Behavior of Steel Pipe Piles

Zhaohui “Joey” Yang<sup>1</sup>, Feng Xiong<sup>2</sup>, Gang Xu<sup>3</sup>, J. Leroy Hulse<sup>4</sup> and Elmer E. Marx<sup>5</sup>

<sup>1</sup> Associate Professor, Dept. of Civil Engineering, University of Alaska Anchorage, Anchorage, Alaska, USA, [afzy@uaa.alaska.edu](mailto:afzy@uaa.alaska.edu)

<sup>2</sup> Assistant Professor, Dept. of Civil Engineering, University of Alaska Anchorage, Anchorage, Alaska, USA, [affx@uaa.alaska.edu](mailto:affx@uaa.alaska.edu)

<sup>3</sup> Graduate Student, Dept. of Civil Engineering, University of Alaska Anchorage, Anchorage, Alaska, USA, [asgx@uaa.alaska.edu](mailto:asgx@uaa.alaska.edu)

<sup>4</sup> Professor, Dept. of Civil & Environmental Engineering, University of Alaska Fairbanks, Fairbanks, Alaska, USA, [ffjlh@uaf.edu](mailto:ffjlh@uaf.edu)

<sup>5</sup> Bridge Design Engineer, State of Alaska DOT & PF-Bridge Section, Juneau, Alaska, USA, [elmer.marx@alaska.gov](mailto:elmer.marx@alaska.gov)

### ABSTRACT :

Frozen ground is significantly stiffer than unfrozen ground. For bridges supported on deep foundations, the bridge stiffness is also measurably increased in the winter months. Significant changes in the bridge pier boundary conditions due to seasonal freezing requires additional detailing to ensure a ductile performance of the bridge during the design earthquake event. Currently, there are no design guidelines for including the effects of seasonal freezing in seismic analysis. A project has been initiated to systematically investigate the effects of seasonal freezing on the seismic behavior of bridges in cold regions. This paper presents the numerical simulation results of an extended reinforced concrete-filled steel pipe pile-shaft system that is to be tested in outdoor conditions. By using the OpenSees computational platform, a nonlinear three-dimensional Finite Element model is established to investigate seasonal freezing effects on the lateral behavior of the soil-pile system. Pushover analysis of the soil-pile system embedded in the experimental site has been performed to predict its lateral behavior. The results demonstrate that the effects of seasonal freezing have a significant impact on the lateral yield force and displacement capacity of the soil-pile system. The location and rotation of plastic hinges are also greatly affected.

### KEYWORDS:

Seasonal Freezing, Soil-Structure Interaction, Finite Element Modeling, Lateral Behavior, Seismic, Bridge

### 1. INTRODUCTION

Seasonally frozen ground is significantly stiffer than unfrozen ground due to the ice matrix formed during freezing. Stevens (1973) found that the stiffness of soils can change by as much as two orders of magnitude when frozen. By conducting dynamic pile tests in the field, Vaziri and Han (1991) found that the presence of a frozen soil layer, even at a modest thickness of less than 0.5 m, could significantly influence the dynamic responses of piles. For bridges supported on deep pile group foundations, the overall bridge stiffness was found to increase measurably in winter months (Yang et al., 2007). As bridge stiffness increases, seismic demand increases significantly (Sriharan et al., 2007; Suleiman et al., 2006). However, there is no systematic study of lateral pile behavior considering seasonal freezing nor are there design guidelines to address these effects.

A project investigating the effects of seasonal freezing on the seismic behavior of bridges in cold regions has been initiated. As an integral part of this project, a set of reinforced concrete-filled steel pipe piles embedded in soils experiencing seasonal freezing will be tested in an outdoor environment. Prior to performing the field

tests a numerical simulation has been conducted. The results of the simulation are presented in this paper.

## 2. DESCRIPTION OF THE SOIL-PILE SYSTEM

### 2.1. Site Description

The proposed test site is located in Fairbanks, Alaska. Permafrost occurs at 5 m below the ground surface. The maximum depth of seasonally frozen soils in Fairbanks varies depending on surface condition, and is typically 1.5 to 3.0 m. The boring log information taken from the geotechnical investigation report is provided schematically in Figure 1. A silt layer extends to the depth of 3 m from the ground surface, which is underlain by a layer of sand with the thickness of 2.9 m; following that is a gravelly sand layer and a gravel layer. Based upon the moisture changes at the ground surface and the partially frozen soil between seasonally frozen layer and the unfrozen layer, transition layers of 0.2 m thickness are assumed for the surface soil and the soil between seasonally frozen layer and the unfrozen layer, as shown in Figure 1.

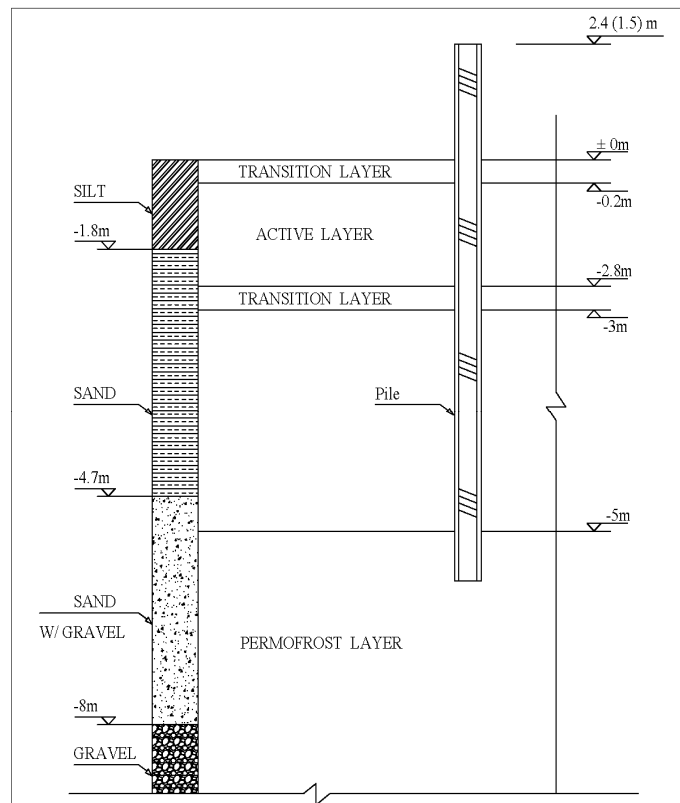


Figure 1 Soil profile of the test site

### 2.2. Test Pile Configuration

A reinforced concrete-filled steel pipe pile is chosen since it is widely used for bridge foundations in the State of Alaska. The pile diameter and reinforcement configuration are determined considering the limitation of the loading equipment and the common practice in Alaska. The test pile specimen configuration is summarized in Table 1. Two test piles and a reaction pile will be constructed on the site in the summer of 2008. One test pile will be tested in summer season of 2008 and the other at the end of winter season of 2009. Each pile will be loaded cyclically to failure using a standard three-cycle, displacement demand protocol.

Table 1 Test pile configuration

Parameter	Value
Total Pile Length	8.4 m
Pile Length Above the Ground Surface	2.4 m
Pile Embedment	6 m
Outside Pipe Diameter	406 mm
Number of Reinforcing Bars	8
Pipe Wall Thickness	9.5 mm
Reinforcing Steel Bar Diameter	19 mm (#6)
Load Point Height (above the ground)	2.4 m

### 3. SIMULATION OF THE SOIL-PILE SYSTEM

#### 3.1. Simulation Platform

The Open System for Earthquake Engineering Simulation (OpenSees) is a software framework for simulating the seismic response of structural and geotechnical systems (Mazzoni et al., 2006; <http://opensees.berkeley.edu/index.php>). OpenSees is emerging as an excellent research tool in studying soil-structure interaction and is chosen for this study. Specifically, a user-friendly GUI developed for soil-pile interaction analysis with OpenSees by Lu et al. (2008), named OpenSeesPL, is used in this analysis.

#### 3.2. Finite Element Model of the Soil-Pile System

A three-dimensional Finite Element model of the soil-pile system is created with OpenSeesPL and shown in Figures 2a, b and c. The model dimensions are 100 m (longitudinal) x 50 m (transverse) x 14 m (vertical). The bottom of the soil domain is 7m below the pile tip. Figure 2a and 2b show the isometric view of the model and the approach of pile-soil coupling, respectively. The reinforced concrete-filled steel pipe pile is modeled using a fiber model having a cross section shown in Figure 2c. The area of cover patch represents the steel pipe; core patch represents the concrete core and the steel layer is used to model the presence of reinforcement bars. The soils are modeled by solid elements. Rigid links, as can be seen from Figure 2b, are applied to connect beam elements with the solid elements in order to account for the pile size effects. Between the pile and the soils, an interface layer has been used to model possible pile installation effects. Properties of the material models are provided in the following sub-sections.

The following boundary conditions are used in the analyses: (1) the bottom of the soil domain is fixed in the longitudinal (X), transverse (Y), and vertical (Z) directions; (2) Left, right and back planes of the model are fixed in X and Y directions (horizontal directions) and free in Z direction; (3) Plane of symmetry is fixed in y direction and free in Z and X direction. Push-over analysis is used to evaluate the pile behavior. Lateral displacement is applied at the pile head in X direction to simulate lateral loading.

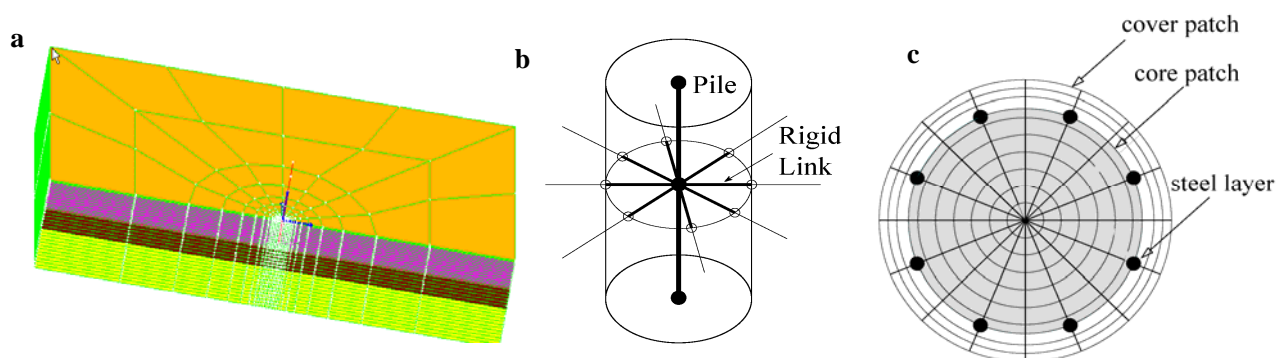


Figure 2 Finite element model of the soil-pile system: (a) Isotropic view; (b) pile-soil coupling by rigid links; (c) fiber sections of the steel pipe pile

#### 3.3. Pile Material Modeling

An enhancement in the flexural strength and ductility of the pile element can be expected due to the increase in concrete compressive strength and crushing strain resulting from the confining action of the steel pipe. To account for the confining effect, the constitutive model developed by Mander et al. (1988) is used for the concrete core. In this model, the increase in concrete compressive strength in the presence of lateral pressure

may be written as:

$$f'_{cc} = f'_{co} \left( 2.254 \sqrt{1 + \frac{7.94 f'_l}{f'_{co}} - \frac{2 f'_l}{f'_{co}}} - 1.254 \right) \quad (1)$$

where,  $f'_{cc}$ ,  $f'_{co}$  are the confined and unconfined compressive strengths of concrete, respectively, and  $f'_l$  the effective lateral confining pressure exerted on the core concrete by the steel pipe at yield. The unconfined compressive strength of concrete at  $-1^\circ\text{C}$  is taken as 45.5 MPa based on the results obtained by Sritharan et al. (2007). The confined compressive strength calculated by Eqn. (1) is 93.5 MPa. The crushing strain also increases from 0.004 for unconfined concrete to 0.02 for well confined concrete. The steel material is modeled by the bilinear model. Table 2 summarizes the material properties of steel and core concrete used in this study.

Table 2 Material properties of steel and confined concrete

OpenSees Model Name	Model parameter	
	Name	Value
Concrete01	Compressive strength (\$fpc)	-93.5 MPa
	Strain at maximum strength (\$epsc0)	-0.0125
	Crushing strength (\$fpcu)	-90.0 MPa
	Strain at crushing strength (\$epsu)	-0.02
Steel 01 (ASTM A706 reinforcement bars)	Yield strength (\$Fy)	470 MPa
	Initial elastic tangent (\$Eo)	200 GPa
	Strain-hardening ratio (\$b)	0.005
Steel 01 (ASTM A53 Grade B Steel pipe)	Yield strength (\$Fy)	335 MPa
	Initial elastic tangent (\$Eo)	200 GPa
	Strain-hardening ratio (\$b)	0.005

### 3.4. Soil and Soil-Pile Interface Modeling

Based on testing results obtained by Vinson et al (1981), the stiffness of frozen silt is dependent on temperature, water/ice content, unfrozen water content, confining pressure, etc. The shear wave velocity ( $V_s$ ) of frozen silt soils from the same area as the test site was found to be around 1,500 m/s by laboratory testing. In-situ testing found that  $V_s$  of naturally frozen silty soils varies from 900 to 1,750 m/s (LeBlanc et al., 2004). Based on these available data, the main layer of seasonal frost (shown as Active Layer in Figure 1) is assumed to be fully frozen with  $V_s$  from 900 to 1,500 m/s, and for permafrost  $V_s$  is 1250 m/s.  $V_s$  of the transition layers at the top is taken as a half of that for fully frozen soil, i.e. 750m/s for reasons discussed in Section 2.1. That for unfrozen silt in this profile is assumed to be 200 m/s based on available data. The shear wave velocity profile used in this analysis is shown in Figure 3.

Both unfrozen and frozen soils are modeled with a Multi-yield surface soil model (Yang et al., 2003). This model can simulate both cohesionless and cohesive soil material behavior with reasonable accuracy. The soil-pile interface needs to be modeled properly in order to simulate the soil-pile interaction under lateral loading with a reasonable accuracy. Possible approaches include special interface elements and soil material models which only allow strength under compression (e.g. Drucker-Prager material model). In this study, the latter approach is adopted. Frozen soil properties were based on the test results obtained by Zhu and Carbee

(1984). The soil material properties in frozen and unfrozen status are listed in Table 3.

Table 3 Material properties of Soils

	Frozen	Unfrozen	Soil-pile interface (frozen)	Soil-pile interface (unfrozen)
Mass density (kg/m <sup>3</sup> )	1.9x10 <sup>3</sup>	1.9x10 <sup>3</sup>	1.9x10 <sup>3</sup>	1.9x10 <sup>3</sup>
Reference shear wave velocity (m/s)	750-1,500	200	600-1,000	200
Cohesion (kPa)	100	0	0	0
Friction Angle (°)	27	33	30	25
Peak shear strain (%)	1	10	1.5	10%

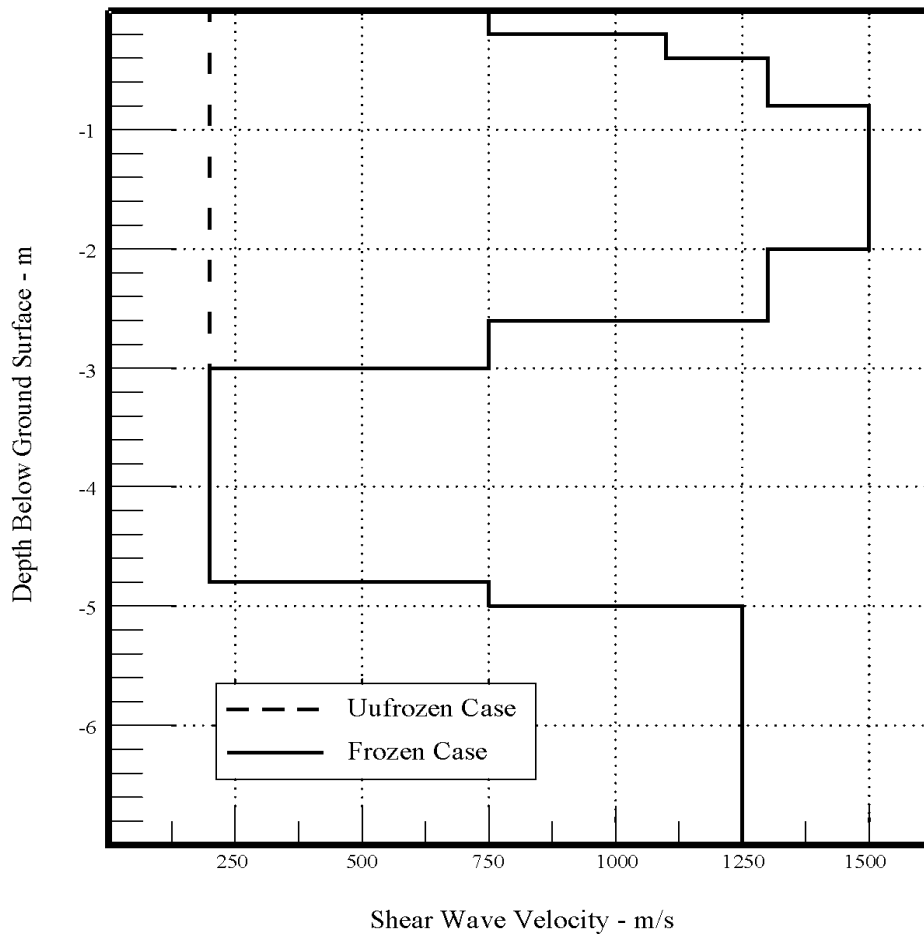


Figure 3 Shear wave velocity profile of the test site

## 4. SIMULATION RESULTS AND DISCUSSION

### 4.1. Pile Section Behavior

Moment-curvature analysis is conducted for the pile section to assess the pile section behavior and the results are shown in Figure 4. The ultimate moment is defined as the moment when the strain in the extreme compression concrete fiber reaches the crushing strain (0.02). It is seen from Figure 4 that the ultimate moment is 420 kN-m. The yield moment, defined as the moment when the strain in the extreme tension steel fiber reaches first yield, is 238.7 kN-m. The ultimate curvature reaches 0.277 rad/m when the strain of the extreme concrete fiber reaches the crushing strain, as seen in Figure 4.

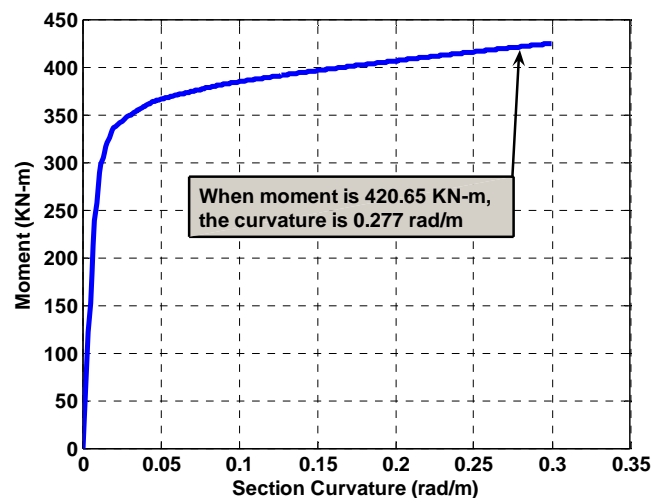


Figure 4 Moment-curvature relationship of the reinforced concrete-filled steel pile section

### 4.2. Pile Behavior

The pile behavior including lateral force vs. displacement, bending moment, shear force and deflection vs. depth obtained at frozen and unfrozen conditions are shown in Figures 5, 6, 7, and 8. With the pile lateral yield lateral force ( $V_y$ ) defined as the lateral load when the strain in the extreme tension steel fiber reaches first yield, it is observed from Figure 5 that the  $V_y$  increases and the lateral displacement capacity at the pile head decreases with the presence of frozen soil. The  $V_y$  increases from 75.8 kN at unfrozen status to 99.5 kN at frozen status, or 31% increase; the displacement capacity at the  $V_y$  decreases from 0.1 m at unfrozen status to 0.03 m at frozen status, or 70% reduction.

Figures 6, 7 and 8 show the bending moment, shear force and deflection versus depth for both frozen and unfrozen conditions at a pile head deflection ( $D_x$ ) of 0.3 m. As before, significantly different pile behaviors for unfrozen and frozen conditions are observed. It is seen from Figure 6 that the locations of maximum moments are founded to be 1.1 and 0.15 m (or 2.75 and 0.38\*Pile Diameter) below ground surface for unfrozen case and frozen case, respectively. From Figures 7 and 8, significant difference is observed in the lateral load and deflection for unfrozen and frozen cases. A comparison of pile behaviors in these two cases is summarized in Table 4. It is also observed in Figures 6 that the bending moment profile of unfrozen case is much larger in the plastic hinge region than that of frozen condition, demonstrating that the plastic hinge length is reduced in the frozen condition. Thus, the plastic hinge rotation and plastic deflection are also reduced.

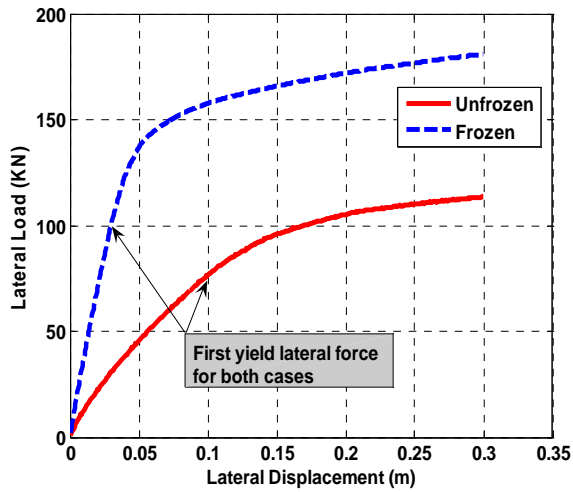


Figure 5 Lateral load vs. deflection

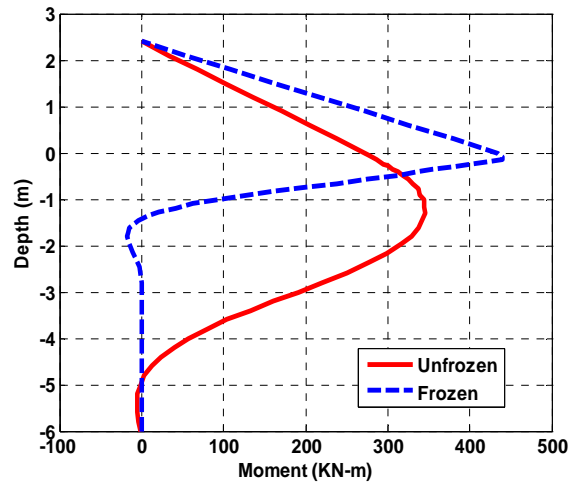


Figure 6 Bending moment vs. depth (Dx=0.3 m)

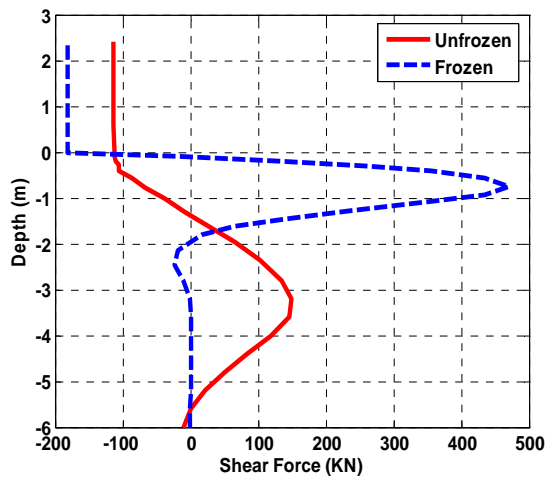


Figure 7 Shear force vs. depth (Dx=0.3 m)

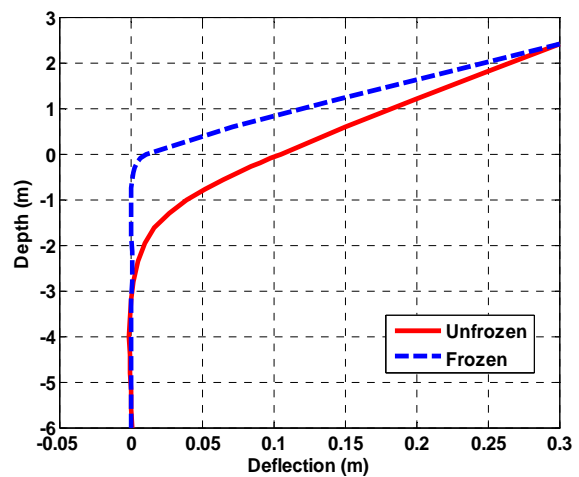


Figure 8 Pile deflection vs. depth (Dx=0.3 m)

Table 4 Comparison of pile behavior at unfrozen and frozen conditions (Dx = 0.3m)

	Lateral Force at Pile Head (KN)	Max. Bending Moment (KN-m)	Max. Bending Moment Depth (m)
Frozen	181	440	0.15 (0.38*Diameter)
Unfrozen	113.5	345	1.1 (2.75*Diameter)

## 5. SUMMARY

This paper presents the results obtained from numerical simulation of the lateral behavior of a soil-pile system under the influence of seasonal freezing. The OpenSees simulation platform is used to conduct pushover analyses for the soil-pile system at both unfrozen and frozen conditions. Results show that seasonal

freezing has great impact on the lateral behavior of the soil-pile system. The pile lateral yield force increases by 31%, and the displacement capacity at the lateral yield force decreases 70%. The maximum bending moment location and plastic hinge location move upward considerably when seasonal freezing occurs. Results also indicate that the plastic hinge length is reduced under the frozen soil condition. It is noted that the numerical simulation results will help establish a testing procedure for the outdoor testing. These results will also be compared with those from the in-situ test to confirm the validity of the model.

## ACKNOWLEDGEMENT

This project is jointly funded by Alaska University Transportation Center (AUTC) and Alaska State Department of Transportation and Public Facilities (AK DOT & PF). This support is gratefully acknowledged. The authors are thankful to Dr. Jinchi Lu, Assistant Research Scientist at the University of California, San Diego for the help provided regarding the use of OpenSeesPL.

## REFERENCES

- Clarke, M.J. and G.J. Hancock. (1990). A study of incremental-iterative strategies for non-linear analyses. *Inter. J. Numerical Methods in Engineering*. **29**, 1365-1391.
- Czajkowski, R.L. and T.S. Vinson (1980). Dynamic properties of frozen silt under cyclic loading. *J. Geotechnical Engineering Division*. 106:GT9, 963-980.
- LeBlanc, A.M., R. Fortier, M. Allard, C. Cosma and S. Buteau. (2004). Seismic cone penetration test and seismic tomography in permafrost. *Can. Geotech. J.* **41**, 769-813.
- Lu, J., Yang, Z., and Elgamal, A. (2008). OpenSeesPL Three-Dimensional Lateral Pile-Ground Interaction, User's Manual, Version 1.00. *Report No. SSPR-06/03*, Department of Structural Engineering, University of California, San Diego.
- Mander, J.B., M.J.N. Priestley and R. Park. (Aug. 1988). Observed stress-strain behavior of confined concrete. *Jour. Struct. Div., ASCE*, **114:8**, 1827-1849.
- Mander, J.B., M.J.N. Priestley and R. Park. (Aug. 1988). Theoretical stress-strain model for confined concrete. *Jour. Struct. Div., ASCE*, **114:8**, 1804-1826.
- Mazzoni, S., F. McKenna, M.H. Scott and G.L. Fenves, et al. (2006). Open System for Earthquake Engineering Simulation User Command-Language Manual. University of California, Berkeley. (<http://opensees.berkeley.edu/OpenSees/manuals/usermanual/index.html>)
- Stevens, H.W. (1973). Viscoelastic properties of frozen soils under vibratory loads. *North American Contribution to the Second International Conf. on Permafrost*, pp. 400-409. Yakutsk, U.S.S.R.
- Sritharan, S., M.T. Suleiman and D. J. White. (February 2007). Effects of seasonal freezing on bridge column-foundation-soil interaction and their implications. *Earthquake Spectra* **23:1**, 199-222.
- Suleiman, M.T., S. Sritharan and D.J. White (2006). Cyclic lateral load response of bridge column-foundation- soil systems in freezing conditions. *Journal of Structural Engineering*. **132:11**, 1745-1754.
- Vaziri, H. and Y. Han. (1991). Full-scale field studies of the dynamic response of piles embedded in partially frozen soils. *Can. Geotech. J.* **28**, 708-718.
- Yang, Z., A. Elgamal, and E. Parra. (2003). A Computational Model for Cyclic Mobility and Associated Shear Deformation. *J. of Geotechnical and Geoenvironmental Engineering*. **129:12**, 1119-1127.
- Yang, Z., U. Dutta, D. Zhu, E. Marx and N. Biswas (2007). Seasonal frost effects on the soil-foundation-structure interaction system. *J. of Cold Regions Engineering*. **21:4**, 108-120.
- Zhu, Y. and D.L. Carbee (1984). Uniaxial compressive strength of frozen silt under constant deformation rates. *Cold Regions Science and Technology*. **9**, 3-15.